Effect of Surface Treatment and Testing Temperature on Mode I Interlaminar Fracture Behavior of Glass Woven Fabric Composites

M.Kotaki[1], T.Kuriyama[1], H.Hamada[2], Z.Maekawa[2] and I.Narisawa[1]

[1]*Department of Polymer Science and Engineering, College of Engineering, Yamagata University, Jonan, Yonezawa 992-8510, Japan*

[2]*Advanced Fibro Science, Kyoto Institute of Technology, Matsugasaki, Sakyo-ku, Kyoto 606-8585, Japan*

ABSTRACT

Mode I interlaminar fracture toughness tests were carried out at room temperature, 60 °C and 100 °C by using double cantilever beam (DCB) specimens with plain glass woven fabric / vinyl ester resin composites. Three types of composites reinforced with glass woven fabrics treated with different silane concentration were used. The mode I fracture toughness for the onset of initial crack propagation increased with increase of testing temperature, and the fracture toughness at high temperature increased with increasing silane concentration, whereas the fracture toughness at room temperature decreased with increasing silane concentration.

1. INTRODUCTION

Environmental effects, such as temperature, moisture and chemical effects, on mechanical properties of polymer composites are significant, important problems for the practical applications of composite materials. Due to the rapidly expanding application of composite materials in many engineering constructions, the issues of the environmental effects are a major concern in design and manufacture of composite materials. Several developments of reinforcement fibers and matrix resins for composite materials with high environmental resistance have been successful, and many investigations have been published in these fields, such as temperature dependence /1,2,3,4,5,6/, thermal degradation behavior /7,8,9,10/, moisture dependence including hot water degradation behavior /11,12,13,14,15/ and chemical degradation behavior /16/.

Woven fabric composites have been widely used in composite fields, especially as printed circuit boards in the electronics industry. The most important performance required in the printed circuit boards is heat resistance as well as dimensional stability and the resin impregnation, because interlaminar delamination and debonding between glass fiber fabrics and matrix resin often occur by the thermal effect during printed wiring manufacturing process. Also for other applications of the woven fabric composites, delamination occurs due to mechanical stress. In practical applications, the delamination between plies is a fatal problem; as it is for the other laminated type composites.

Many works have investigated the delamination behavior of laminated composites, especially for unidirectional laminates since the 1980s. To improve delamination resistance, several thermoplastic resins /17,18,19,20/ and rubber-modified epoxies /21,22, 23,24/ have been used as matrix resin, and also other techniques such as interleaving /25,26/ and stitching /27,28/ have also been successful. Several investigations have also been conducted on the delamination behavior of woven fabric composites with higher delamination resistance compared to unidirectional composites /29,30,31,32,33,34,35/. These

papers were mainly concerned with the effects of weaving pattern and delamination direction, and very few papers dealt with interfacial adhesion between fiber and matrix, even though the interfacial adhesion greatly affects the mechanical properties of composite materials.

Concerning the effects of temperature on delamination behavior of polymer composites, several works have been reported in unidirectional composites /2,3,4/ and woven fabric composites /1/. Leach and Moore /2/ reported the temperature dependence of the delamination behavior of carbon/PEEK composites, in comparison between comparative (damage resistance to impact loading) and intrinsic toughness (mode I interlaminar fracture toughness). Hine and other co-wokers /3/ reported that mode I interlaminar fracture toughness of unidirectional carbon/PEEK composites was mainly related to the contributions from matrix deformation and fiber bridging. They also reported that the poor interfacial adhesion between fiber and resin led to relatively low fracture toughness that was independent of temperature in the unidirectional carbon/PEEK material system /4/. The mechanisms of mode I interlaminar fracture behavior of woven fabric composites at high temperature were not well identified, especially in terms of interfacial adhesion effects.

The effects of interfacial adhesion on the mode I and mode II interlaminar fracture behavior of plain glass woven fabric composites were investigated in a series of this work /36/, and the mechanism of mode I interlaminar fracture of the woven fabric composites was identified on the basis of detailed microscopic observation of the crack tip. In the present study, mode I interlaminar fracture behavior at high temperature for plain glass woven fabric composites was investigated with emphasis on the effect of interfacial adhesion between fiber and resin on the fracture behavior.

2. EXPERIMENTAL DETAILS

2.1 Materials

Materials used in this paper were plain glass woven fabrics of 44(warp)x34(weft) strands count over inch (WE18W: Nitto Boseki Co., Ltd., Japan) as reinforcement. The fiber strands from the E-glass fiber fabric consisted of 400 glass fiber filaments of 9 μm diameter. Surface treatment was performed on the glass fiber fabrics using γ-methacryloxypropyltrimethoxy-silane (A-174: Nippon Unicar Company, Japan) referred to as MPS. The aqueous solutions of MPS were acidified with acetic acid at pH = 4.0. The glass fiber fabrics were dipped into the MPS aqueous solutions. They were squeezed between squeeze rollers and dried at 110 °C for 10 min. The concentrations of MPS used were 0.01, 0.4 and 1.0 wt%.

The matrix resin used in this study was a bisphenol-A type vinyl ester resin (R-806; Showa Highpolymer Co., Ltd., Japan), which included styrene monomer of approximately 45wt%. The room temperature catalyst used was 0.7 phr methylethylketoneperoxide (MEKPO) promoted by 0.3 phr cobalt naphthenate solution. Twenty-ply composite laminates with 4mm thickness were fabricated by the hand lay-up technique. The composite laminates were cured at 80°C for 3h and at 150°C for 2h after being at room temperature for 48h. The volume fraction of fiber for the laminates was approximately 40 %.

2.2 Fracture Toughness Tests

Mode I interlaminar fracture toughness tests were performed with DCB specimens as shown in Fig.1. The DCB specimens were cut parallel to the weft fiber direction, with 100 mm length and 25 mm width. Initial defects of the DCB specimens were introduced by inserting PTFE film 40 μm thick during molding of the laminates. Mode I interlaminar fracture toughness tests were carried out under a stroke rate of 1.0 mm/min by using a Shimadzu Autograph universal testing machine at room temperature, 60 °C and 100 °C. The crack lengths at room temperature were measured on one side of the specimen with a traveling microscope at a magnification of x100 during the testing. Displacement of the testing machine was used as the crack opening displacement (COD) on the load line. Mode I interlaminar fracture toughness values were calculated in accordance with JIS K7086 as follows:

$$G_{IC,R} = \frac{3P_c^2 (B\lambda)^{2/3}}{2(2H)B^2 \alpha_1} \quad (1)$$

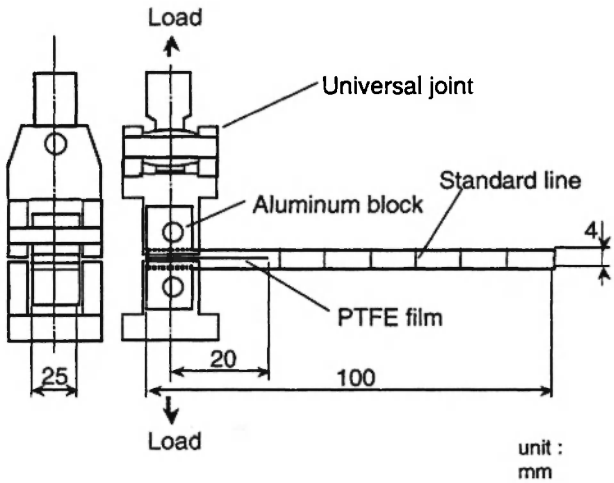

Fig. 1: DCB specimen and loading apparatus.

where: λ = compliance; H = half thickness; B = specimen width; P_c = critical load; and α_1 = empirical parameter. At room temperature, the empirical parameter α_1 was determined by following equation:

$$\frac{a}{2H} = \alpha_1 (B\lambda)^{1/3} + \alpha_0 \quad (2)$$

where: a = measurement crack length; and α_0 = empirical parameter. At 60 °C and 100 °C, the empirical parameter α_1 was derived as follows:

$$\alpha_1 = 10 D_1 (E_L)^{1/3} \quad (3)$$

where: $D_1 = 0.25$; and E_L = bending modulus.

3. RESULTS

Fig. 2 shows typical load-COD curves of the DCB tests at different testing temperature for plain glass woven fabric composites. For the 0.01wt% specimens, the loads increased through a non-linear point to a maximum point followed by a gradual decrease with further crack extension. The crack propagated in a slow and stable manner at all temperatures. In sharp contrast, for the 0.4wt% specimens, the load-COD curves displayed saw teeth like behavior at room temperature, where the rising portion and the abrupt drop of the load corresponded to stable crack re-initiation and crack arrest after rapid crack propagation, respectively. On the other hand, at 60 °C and 100 °C, the load gradually decreased after maximum load, and then the crack

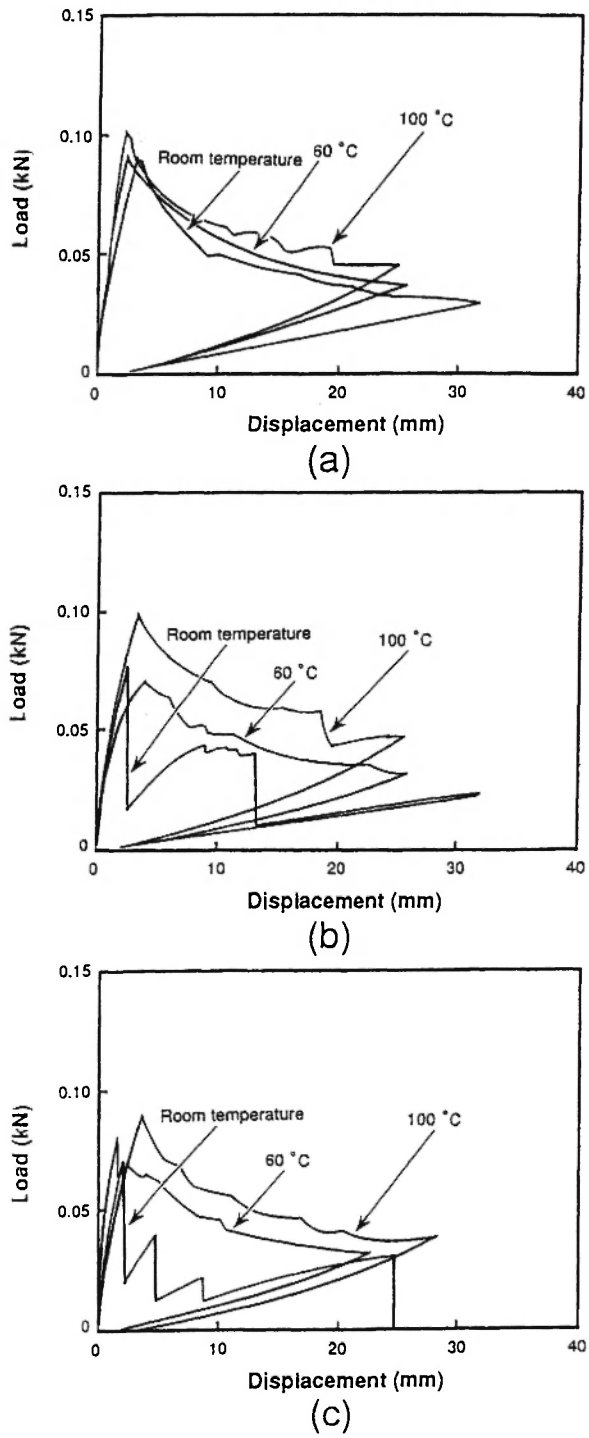

Fig. 2: Typical load-COD curves in plain glass woven fabric composites; (a) MPS 0.01wt%, (b) MPS 0.4wt% and (c) MPS 1.0wt%.

propagated slowly and in a stable manner. Consequently, the crack growth behavior changed from an unstable to a stable manner with increasing testing temperature in the 0.4wt% specimens. With the 1.0wt% specimens, the fracture behavior changed from unstable to stable fractures with increasing testing temperature similar to the 0.4wt% specimens.

Fig. 3 shows the relation between mode I interlaminar fracture toughness, as determined from equation (1), and crack extension, *R*-curves. The 0.01wt% specimen at room temperature displayed almost constant fracture toughness with increasing crack extension after the initial crack extension. On the other hand, the fracture toughness increased with increasing crack extension at 60 °C and 100 °C. In the 0.4wt% specimen at room temperature, there were some points in the *R*-curves where fracture toughness rapidly decreased, and the R-curve displayed saw-tooth-like behavior. These points where fracture toughness started rapidly to decrease were the onset of the unstable fracture. The fracture toughness displayed almost constant values at 60 °C, but it increased with increasing crack extension at 100 °C. In the 1.0wt% specimens, the *R*-curve displayed the sawtooth-like behavior at room temperature, whereas the fracture toughness showed almost constant values at 60 °C and 100 °C.

In a series of this work /37/, it was identified that the mode I interlaminar crack initiated at the onset of the non-linearity, P_{NL}, and initially propagated at the maximum load point, P_{Max}, in the initial load-displacement curve of DCB tests at room temperature without respect to the MPS concentration for the plain glass woven fabric composites. However, the crack initiation behavior was quite different with change in MPS concentration. In the 0.01wt% specimen, the mode I crack initiated with fiber strands and propagated across the fiber strands with micro-cracks in the fiber strands. On the other hand, in the 1.0wt% specimen, the mode I crack initiated in the resin rich region between plies and propagated into the resin region without micro-cracks. The OM observation was conducted on the crack tip at P_{NL} in the initial load – displacement curve tested at 100°C, in order to confirm the crack initiation point tested at the higher temperature. Fig. 4 shows the OM micrograph of the damage zone ahead of the initial crack tip for the 1.0wt% specimen tested at room

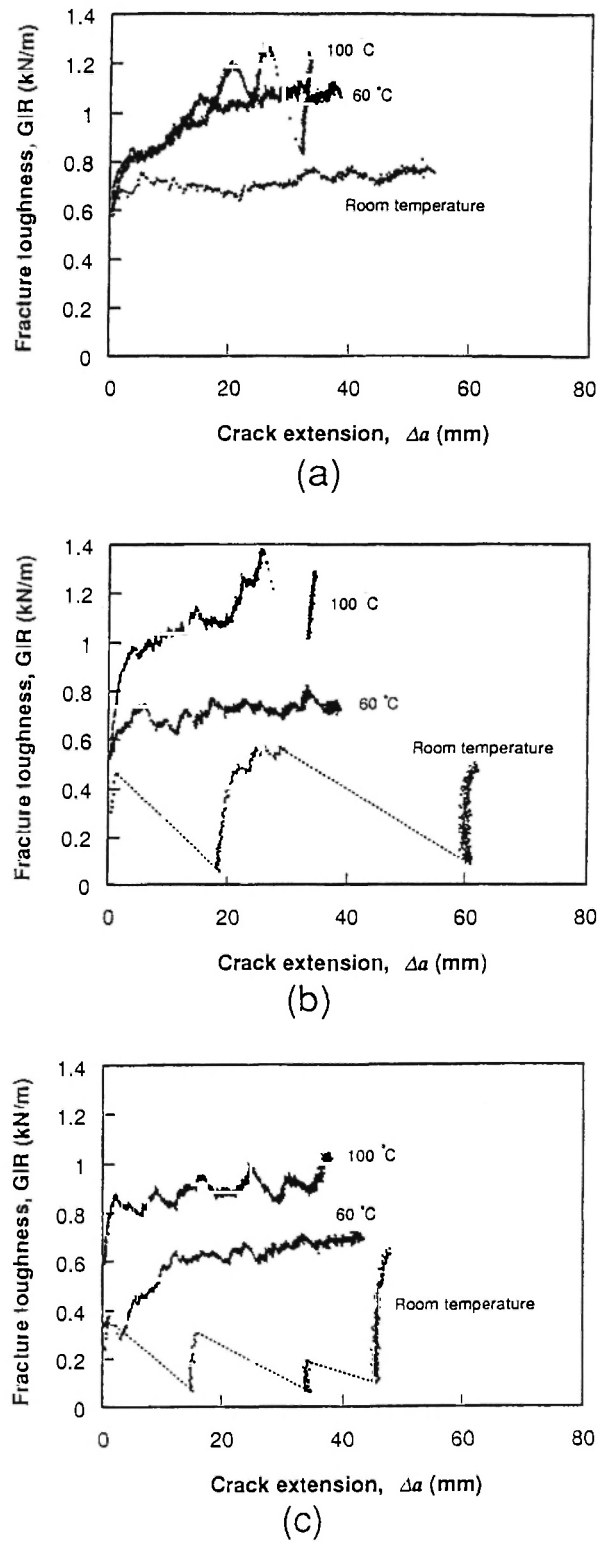

Fig. 3: Relation between mode I interlaminar fracture toughness and crack extension of plain glass woven fabric composites; (a) MPS 0.01wt%, (b) MPS 0.4wt% and (c) MPS 1.0wt%.

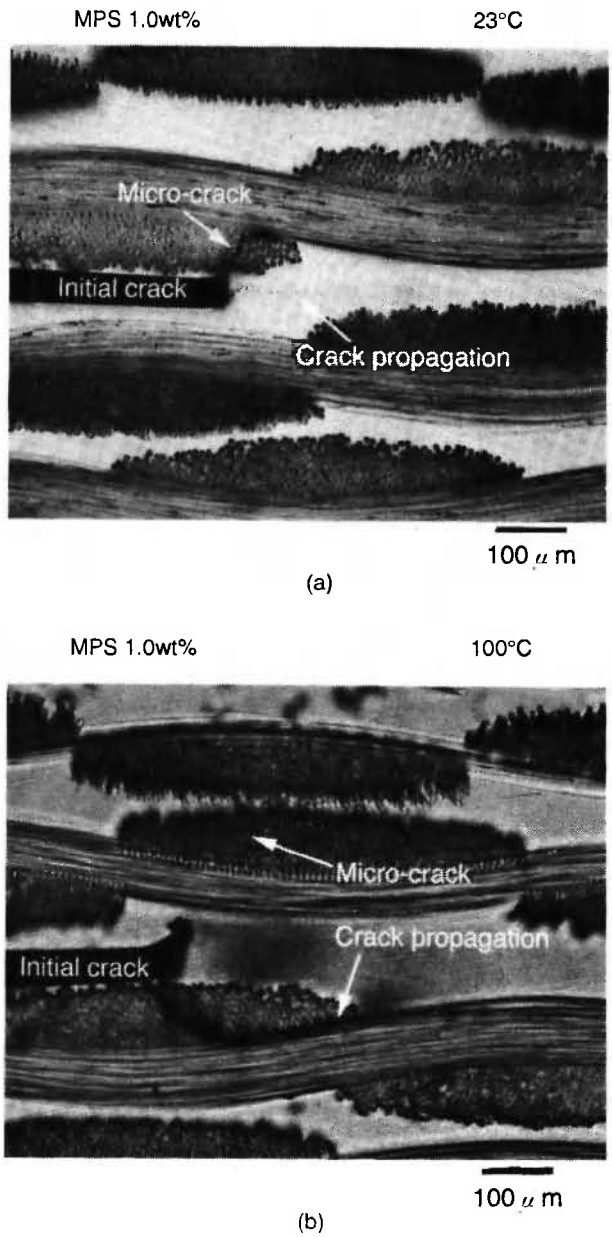

Fig. 4: OM micrographs of the initial crack tip at P_{NL} for MPS 1.0wt% specimen; tested at (a) room temperature and (b) 100°C.

temperature and at 100°C. The mode I interlaminar crack initiated at the tip of the initial crack film at P_{NL} tested at 100°C as well as at room temperature. So, the mode I crack initiation point can be considered to be also at P_{NL} in the initial load – displacement curves tested even at high temperature. However, the crack initiation behavior with the 1.0wt% specimen was different from the case at room temperature. At 100°C, the crack did not initiate into the resin rich region between plies as at room temperature, but propagated to across the fiber strands. The behavior was similar to the 0.01wt% specimen tested at room temperature/37/.

The relation between initiation values of mode I interlaminar fracture toughness and MPS concentration for the plain glass woven fabric composites tested at different temperature is shown in Fig. 5. The initiation

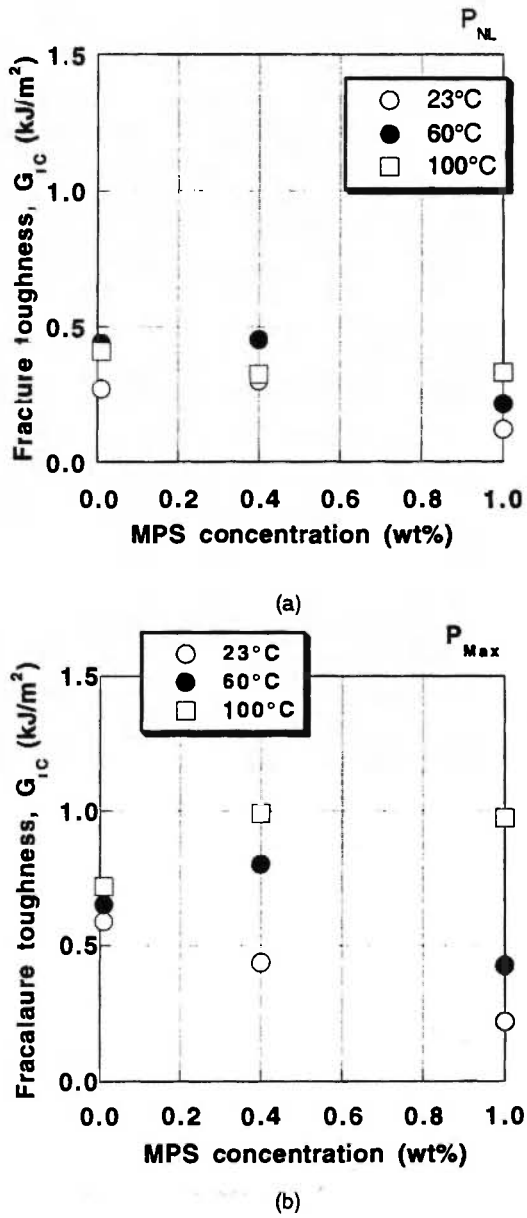

Fig. 5: Relation between initiation values of mode I interlaminar fracture toughness and MPS concentration of plain glass woven fabric composites.

values of mode I interlaminar fracture toughness calculated at P_{NL} tested at room temperature and at 60°C slightly decreased with increasing MPS concentration. However, the significant difference of the fracture toughness at 100°C was not found with increasing MPS concentration. The dependency of the initiation values of mode I interlaminar fracture toughness calculated at P_{Max} to the MPS concentration was very clear compared to that of the fracture toughness at P_{NL}. The initiation values of fracture toughness at P_{Max} increased with increasing testing temperature independent of MPS concentration. The rate of increase of the fracture toughness with increase of testing temperature in the 1.0wt% specimen was much higher than that in the 0.01wt% specimen. In MPS concentration dependency, the fracture toughness tested at room temperature clearly decreased with increasing MPS concentration, however, the fracture toughness tested at 100°C increased with increasing MPS concentration.

The differences of mode I interlaminar fracture toughness between P_{NL} and P_{Max}, ΔG_I, are shown in Fig.6. In a series of this work /37/, it was clear from the OM observation that the ΔG_I was corresponding to the fracture energy for forming the damage zone ahead of the crack tip before the crack propagation. The ΔG_I tested at 100°C was higher than that at room temperature with the higher MPS concentration

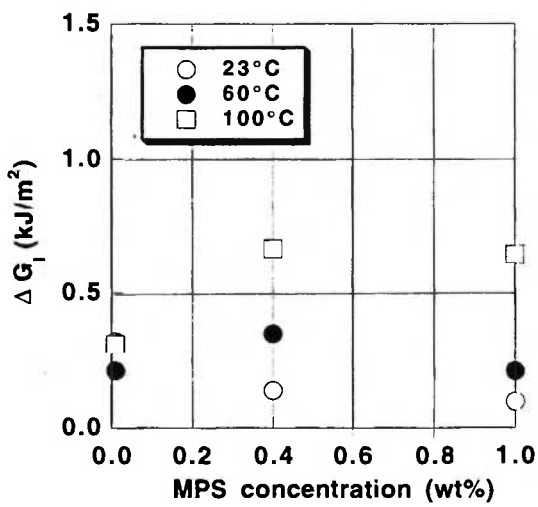

Fig. 6: Difference of mode I fracture toughness between P_{NL} and P_{Max} of plain glass woven fabric composites as a function of MPS concentration.

specimens. And the ΔG_I at 100°C increased with increasing MPS concentration, whereas the ΔG_I at room temperature decreased.

Figs. 7 and 8 show SEM micrographs of the cross sections of DCB specimens for the 0.01wt% and 1.0wt% MPS tested at different temperatures. In the case of the 0.01wt% specimens, the crack propagated across the fiber strands, and multiple cracks such as micro-cracks in the fiber strands and sub-cracks

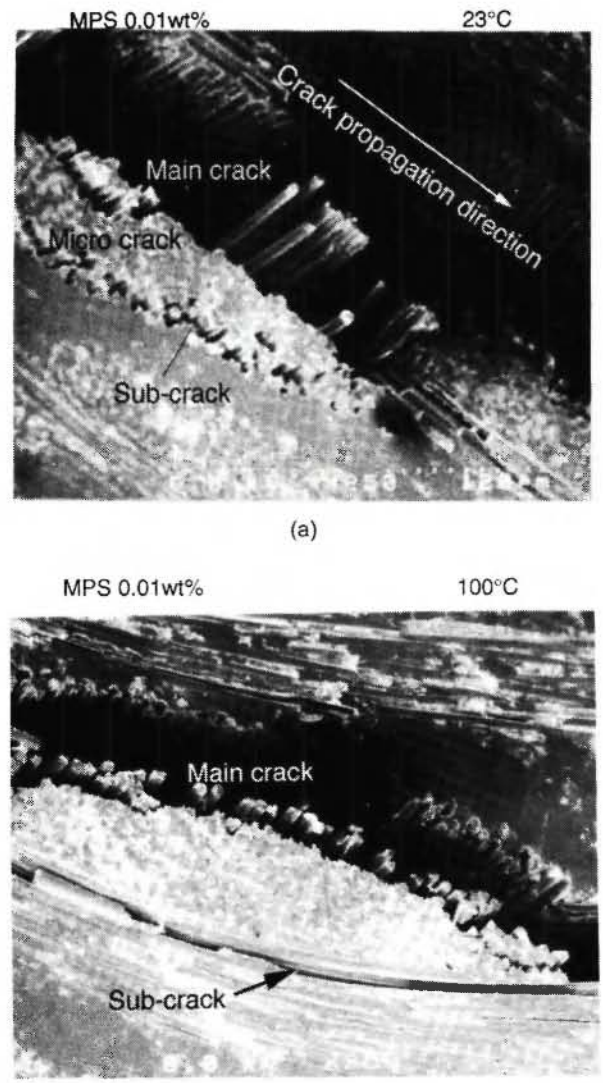

Fig. 7: SEM micrographs of the cross sections of DCB specimens after mode I interlaminar crack propagation for MPS 0.01wt% specimens of plain glass woven fabric composites; tested at (a) 23°C and (b) 100°C

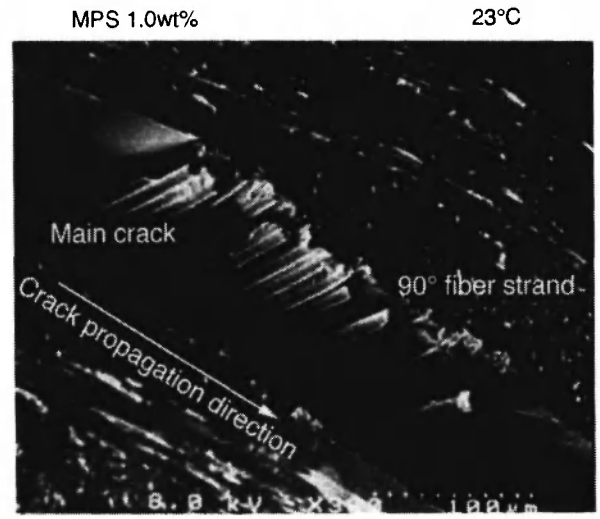

Fig. 8: SEM micrographs of the cross sections of DCB specimens after mode I interlaminar crack propagation for MPS 1.0wt% specimen of glass plain woven fabric composites; tested at (a) 23°C and (b) 100°C

between fiber strands and resin rich region were observed at both room temperature and 100°C. In the 1.0wt% specimens, the crack also propagated across the fiber strands with multiple cracks at 100°C, although the crack ran into the resin rich region between plies at room temperature. The 1.0wt% specimen tested at 100°C showed similar fracture behavior to the 0.01wt% specimen.

SEM micrographs of fiber surfaces on the mode I interlaminar fracture surface tested at different temperatures for the 0.01wt% and 1.0wt% specimens are shown in Figs. 9 and 10. Much more resin adhered on the fiber surface in the 1.0wt% specimen at room temperature, compared to the 0.01wt% specimen. In the SEM observation of the 0.4wt% specimen, a great deal of resin also adhered to the fiber surface at room temperature. The fiber surface treatment with higher MPS concentration leads to the good interfacial adhesion between glass fiber and resin at room

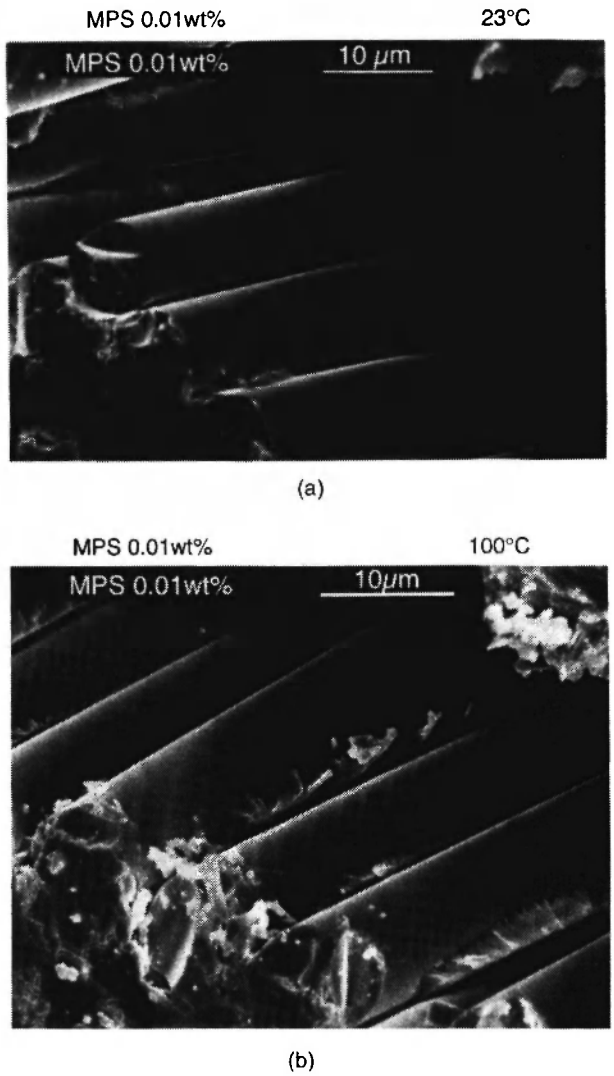

Fig. 9: SEM micrographs of fiber surface on mode I fracture surface of MPS 0.01wt% specimens of plain glass woven fabric composites; tested at (a) 23°C and (b) 100°C.

temperature. However, the morphology of the fracture surface tested at 100°C was completely different from that at room temperature in every type of specimen with different MPS concentration. In the 0.01wt% specimen tested at 100°C, the resin adhered to fiber surfaces and it failed in a brittle manner. In the 1.0wt% specimen, the resin observed on fiber surface showed typical ductile behavior where the resin was elongated and deformed, whereas the resin on the fracture surface tested at room temperature showed brittle behavior. SEM micrographs of the debonding between fiber and matrix resin in a fiber strand on the cross section of DCB specimens tested at different testing temperatures are shown in Fig. 11. The deformation of the matrix resin into an elliptical shape was clearly observed at 100°C compared to the specimen tested at room temperature, and this behavior was independent of MPS concentration.

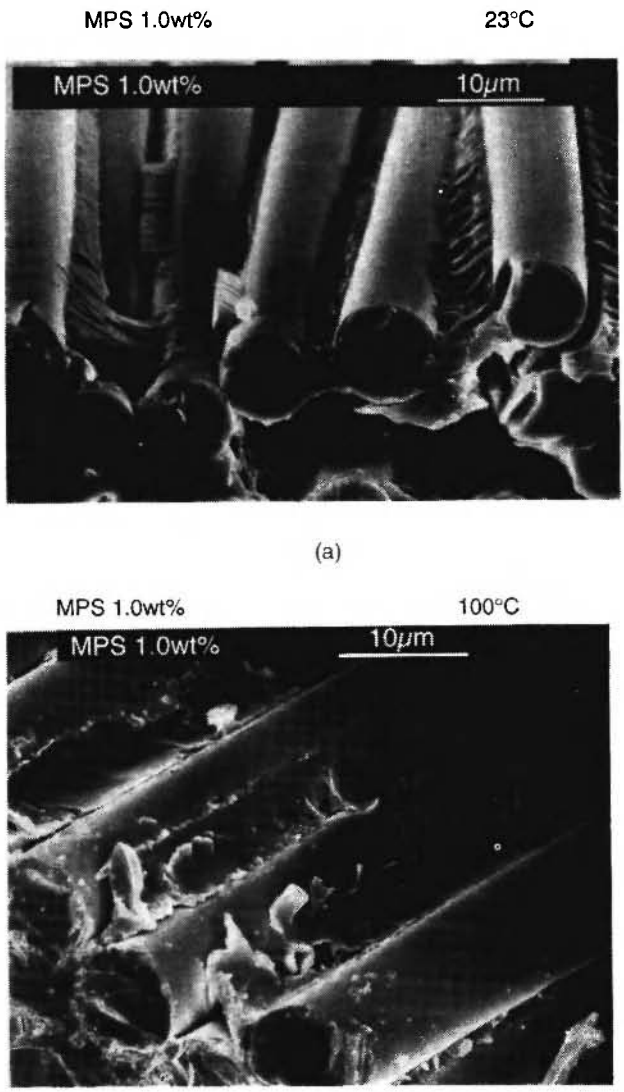

Fig. 10: SEM micrographs of fiber surface on mode I fracture surface of MPS 1.0wt% specimens of plain glass woven fabric composites; tested at (a) 23°C and (b) 100°C.

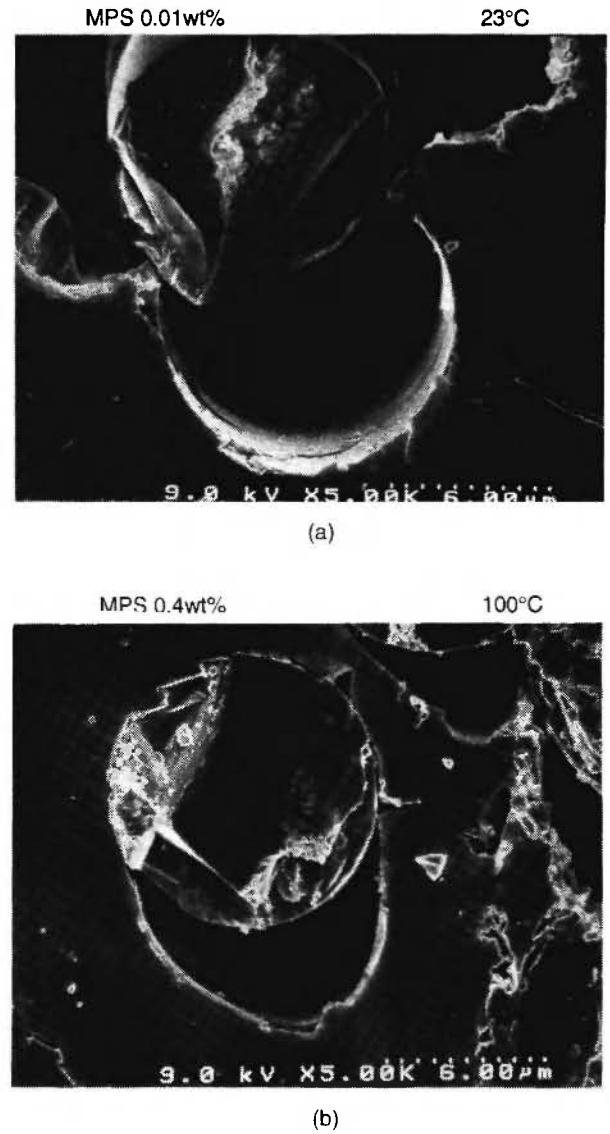

Fig. 11: SEM micrographs of the deformation of matrix resin around fiber in the cross section of DCB specimens; (a) MPS 0.01wt% at room temperature and (b) MPS 0.4wt% at 100°C.

4. DISCUSSION

Mechanisms of mode I interlaminar fracture for plain glass woven fabric composites at room temperature were investigated in a series of this work /37/. The mode I fracture toughness for initial crack propagation decreased with increasing MPS concentration, which was correlated to a damage zone size ahead of the initial crack tip, i.e. a fracture energy for forming micro-cracks in fiber strands. In the low MPS concentration case (poor interfacial adhesion at room temperature), a larger damage zone caused by a number of the micro-cracks was developed ahead of the initial crack tip and a higher fracture toughness was obtained.

The mode I interlaminar fracture behavior of the high MPS concentration specimens changed from an unstable manner with no micro-crack to a stable manner with micro-cracks in fiber strands with increase of testing temperature, even though the low MPS concentration specimen displayed a stable fracture behavior without respect to testing temperature. The mode I fracture toughness for initial crack propagation increased with increasing testing temperature in all types of the specimens with different MPS concentration. This is due to the increase of fracture toughness of the matrix resin /37/. In addition, tor the high MPS concentration specimens, the fracture energy for forming micro-cracks also contributed to the higher fracture toughness at high temperature. This is the reason why the high MPS concentration specimens show larger increment at high temperature compared to the low MPS concentration specimens.

In SEM observations of the fracture surface tested at high temperature, the resin adhering to the fiber surfaces exhibit a brittle manner in the low MPS concentration specimen and a ductile manner in the high MPS concentration specimens. The morphologies of the fracture surfaces indicate a good interfacial adhesion for the low MPS concentration and a poor interfacial adhesion for the high MPS concentration specimens tested at high temperature, which is a different trend from the case at room temperature.

At high testing temperature, the fracture toughness increased with increasing MPS concentration. This is the opposite tendency to the case at room temperature. The MPS concentration dependency on the fracture toughness at high temperature may be due to the same toughening mechanism as at room temperature, in which a poor interfacial adhesion leads to a higher fracture toughness by the contribution of fracture energy required to produce micro-cracks, because the contribution from the deformation energy of the matrix resin to the fracture toughness was independent of the interfacial adhesion between fiber and resin. However, further studies are still required to identify the mechanism of improvement of the interfacial adhesion in the low MPS concentration specimen at high temperature, although it can be considered that the decrease of the interfacial adhesion in the high MPS concentration specimen at high temperature is due to the increase in mobility of silane molecules on the interface between glass fiber and matrix resin.

5. CONCLUSIONS

In this study, mode I interlaminar fracture behavior at high temperature for plain glass woven fabric composites was investigated on the basis of the discussion of the effect of interfacial adhesion between fiber and resin on the fracture behavior.

- Fracture mechanism of woven fabric composites at high temperature
- Temperature dependency on interfacial adhesion

REFERENCES

1. S.L. Bazhenov. Strong bending in the DCB interlaminar test of thin, E-glass woven-fabric-reinforced laminates, *Composites*, **22**(4), 275-280 (1991).
2. D.C. Leach and D.R. Moore Toughness of aromatic polymer composites reinforced with carbon fibers, *Composites Science and Technology*, **23**, 131-161 (1985).
3. P.J. Hine, B. Brew, R.A. Duckett and I.M. Ward. Failure mechanisms in continuous carbon-fiber reinforced PEEK composites, *Composites Science and Technology*, **35**, 31-51 (1989).

4. P.J. Hine, B. Brew, R.A. Duckett and I.M. Ward. Failure mechanisms in carbon fiber reinforced poly(ether ether ketone. II: Material variables, *Composites Science and Technology*, **40**, 47-67 (1991).
5. J.K. Kim and Y.W. Mai. Effects of interfacial coating and temperature on the fracture behaviors of unidirectional Kevlar and carbon fiber reinforced epoxy resin composites, *Journal of Materials Science*, **26**, 4702-4720 (1991).
6. R.D. Kriz. Influence of damage on mechanical properties of woven fabric composites at low temperature, *Journal of Composite Technology and Research*, **7** (1), 55-58 (1985).
7. J.R. Hwang and A.S. Lee. Thermal damage effects on mode II interlaminar fatigue crack propagation of graphite/epoxy composites, *Composite Structures*, **27**, 389-393 (1994).
8. L.J. Burcham, R.F. Eduljee and J.W. Gillespie, Jr. Investigation of the microcracking behavior of bismaleimide composites during thermal aging, *Polymer Composites*, **16** (6), 507-517 (1995).
9. T.F. Walsh and C.E. Bakis. The effect of high-temperature degradation on the mode I critical strain energy release rate of a graphite/epoxy composite, *Journal of Composites Technology and Research*, **17** (3), 228-234 (1995).
10. A. Watt, A. Goodwin and A.P. Mourits. Thermal degradation of the model interlaminar fracture properties of stitched glass fiber / vinyl ester composites, *Journal of Materials Science*, **33**, 2629-2638 (1998).
11. R. Frassine and A. Pavan. The combined effects of curing and environmental exposure on fracture properties of woven carbon/epoxy laminates, *Composites Science and Technology*, **51**, 495-503 (1994).
12. A.J. Russel and K.N. Street. Moisture and temperature effects on the mixed-mode delamination fracture of unidirectional graphite/epoxy, ASTM STP,876, 1985, 349-370.
13. C. Lhymn and M. Pfaff. Effect of moisture and temperature on toughness of polymer composites, ASME PVP, 146, 1988, 109-115.
14. Z.D. Xiang and F.R. Jones. Thermal-spike-enhanced moisture absorption by polymer-matrix carbon-fiber composites, *Composites Science and Technology*, **57**, 451-461 (1997).
15. T. Morii, H. Hamada, Z. Maekawa, T. Tanimoto, T. Hirano and K. Kiyosumi. Weight change mechanism of randomly oriented GFRP panel immersed in hot water, *Composite Structures*, **25**, 95-100 (1993).
16. Y. Fujii, S. Ramakrishuna, H. Hamada, Z. Maekawa, A. Murakami and T. Yoshiki. Estimation of creep damage in GFRP laminates under corrosive environments using acoustic emission, Proceedings of 39th International SAMPE Symposium, 1994, 1356-1367.
17. P.J. Hine, B. Brew, R.A. Duckett and I.M. Ward. Failure mechanisms in carbon-fiber-reinforced poly(ether sulphone), *Composite Science and Technology*, **43**, 37-47 (1992).
18. R.A. Crick, D.C. Leach, P.J. Meakin and D.R. Moore. Interlaminar fracture morphology of carbon fiber/PEEK composites, *Journal of Materials Science*, **22**, 2094-2104 (1987).
19. H. Wittich and K. Friedrich. Interlaminar fracture energy of laminates made of thermoplastics impregnated fiber bundles, *Journal of Thermoplastic Composite Materials*, **1**, 221-231 (1988).
20. M. Hojo and T. Aoki. Thickness effect of double cantilever beam specimen on interlaminar fracture toughness of AS4/PEEK and T800/epoxy laminates, ASTM STP 1156, 1993, 281-298.
21. W.D. Bascom, J.L. Bitner, R.J. Moulton and A.R. Siebert. The interlaminar fracture of organic-matrix, woven reinforcement composites, *Composites*, **11**, 9-18 (1980).
22. J.K. Kim, C. Baillie, J. Poh and Y.W. Mai. Fracture toughness of CFRP with modified epoxy resin matrices, *Composite Science and Technology*, **43** 283-297 (1992).
23. V.K. Srivastava and B. Harris. Effect of particles on interlaminar crack growth in cross-plies carbon-fiber / epoxy laminates, *Journal of Materials Science*, **29**, 548-553 (1994).
24. D.J.-P. Turmel and I.K. Partridge. Heterogeneous phase separation around fibers in epoxy/PEI blends and its effect on composite delamination resistance, *Composite Science and Technology*, **57**,

1001-1007 (1997).
25. A. Aksoy and L.A. Carlsson. Interlaminar shear fracture of interleaved graphite/epoxy composites, *Composite Science and Technology*, **43**, 55-69 (1992).
26. L.Y. Xu and C.H. Kou. Effect of the interfacial interleaf to the interlaminar fracture of a new BMI matrix composites system, *Journal of Reinforced Plastics and Composites*, **13**, 509-540 (1994).
27. A.P. Mouritz, J. Gallapher and A.A. Goodwin. Flexural strength and interlaminar shear strength of stitched GRP laminates following repeated impacts, *Composite Science and Technology*, **57**, 509-522 (1997).
28. L.K. Jain and Y.W. Mai. On the effect of stitching on mode I delamination toughness of laminated composites, *Composite Science and Technology*, **51**, 331-345 (1994).
29. T.W.H. Wang and F.D. Blum. Interfacial mobility and its effect on interlaminar fracture toughness in glass-fiber-reinforced epoxy laminates, *Journal of Materials Science*, **31**, 5231-5238 (1996).
30. J.G. Funk and J.W. Deaton. The Interlaminar Fracture Toughness of Woven Graphite / Epoxy Composites, NASA Technical Paper 2950, 1989, 1-26.
31. B.J. Briscoe, R.S. Court and D.R. Williams. The effects of fabric weave and surface texture on the interlaminar fracture toughness of aramid/epoxy laminates, *Composite Science and Technology*,**47**, 261-270 (1993).
32. V. Chellapa and B.Z. Jang. Crack growth and fracture behavior of fabric reinforced polymer composites, *Polymer Composites*, **17** (3), 443-450 (1996).
33. N. Alif, L.A. Carlsson and L. Boogh. The effect of weave pattern and crack propagation direction on mode I delamination resistance of woven glass and carbon composites, *Composites*, **29B**, 603-611 (1998).
34. B.J. Briscoe and D.R. Williams. Acid-base interactions in the interpretation of aramid composite and fabric mechanics, *Journal of Adhesion Science Technology*, **5**, 23-38 (1990).
35. N. Alif, L.A. Carlsson and J.W. Gillespie, Jr. Mode I, mode II and mixed mode interlaminar fracture of woven fabric carbon / epoxy, ASTM STP 1242, 1997, 82.
36. M. Kotaki, T. Kuriyama, H. Hamada, Z. Maekawa and I. Nariswa. Mode I and mode II interlaminar fracture behavior of glass woven fabric composites, *Science and Engineering of Composite Materials* (in submission).
37. Y. Suzuki. Study on interfacial properties of glass woven fabric laminated composites, PhD. thesis, Kyoto Institute of Technology, 1993.